Table S1. Tropical systems that passed within 200 km of the northern Chandeleur Islands study area between 1979 and 2019. [Abbreviation: TS, tropical storm]

Storm Name	Landfall	Intensity[1]	Distance from study area
Hurricane Bob	11-Jul-1979	1	<160 km W
Hurricane Frederic	13-Sep-1979	4	<40 km E
Hurricane Elena	02-Sep-1985	3	≤40 km NE
Tropical Storm Juan	31-Oct-1985	TS	~40 km SE
Hurricane Florence	10-Sep-1988	1	~80 km SW
Hurricane Opal	04-Oct-1995	4	<160 km SE
Hurricane Danny	18-Jul-1997	1	<40 km S
Hurricane Georges	28-Sep-1998	2	<40 km E
Tropical Storm Hanna	14-Sep-2002	TS	0 km
Hurricane Isidore	26-Sep-2002	TS	<160 km E
Hurricane Ivan	16-Sep-2004	3	<120 km E
Hurricane Cindy	06-Jul-2005	1	<120 km W
Hurricane Katrina	29-Aug-2005	4	<120 km W
Hurricane Gustav	01-Sep-2008	2	~200 km SW
Hurricane Ida	10-Nov-2009	1	~120 km S
Hurricane Isaac	28-Aug-2012	1	~120 km SW
Hurricane Nate	08-Oct-2017	1	<40 km W

[1] Maximum intensity within 200 km of study area.

Table S2. Spectral bands for Landsat 5 Thematic Mapper (TM), 7 Enhanced Thematic Mapper Plus (ETM+), and 8 Operational Land Imaging (OLI) sensors used in this study. All bands are 30-m resolution except for the thermal-infrared band, which is acquired at 60- to 120-m resolution and resampled to 30 m prior to distribution. [Abbreviations: N/A, not applicable; SWIR, short-wave infrared]

Spectral Range	Band (TM, ETM+)	Wavelength (µm)	Band (OLI)	Wavelength (µm)
Coastal aerosol	N/A	N/A	1	0.43-0.45
Visible blue	1	0.45-0.52	2	0.45-0.51
Visible green	2	0.52-0.60	3	0.53-0.59
Visible red	3	0.63-0.69	4	0.64-0.67
Near infrared	4	0.76-0.90	5	0.85-0.88
SWIR 1	5	1.55-1.75	6	1.57-1.65
Thermal Infrared	6	10.40-12.50	10[1]	10.6-11.19
SWIR 2	7	2.08-2.35	7	2.11-2.29
Panchromatic	8[2]	0.52-0.90	8	0.53-0.59
Cirrus	N/A	N/A	9	1.36-1.38

[1] Landsat 8 OLI thermal infrared band 11 (11.50-12.51 µm) was not used in this study.
[2] Panchromatic band N/A on Landsat 5 TM sensor.

Table S3. Source image-acquisition dates used to create reference datasets used in accuracy assessment. [Abbreviations: NLCD, National Land Cover Dataset; BICM, Barrier Island Comprehensive Monitoring program]

Dataset	Image Date(s)
BICM 2016	11-Oct-2016 to 30-Oct-2016
NLCD 2016	18-Jan-2016; 30-Sep-2016
NLCD 2013	24-Oct-2013
NLCD 2011	16-Aug-2011; 3-Oct-2011
BICM 2008	28-Oct-2008; 29-Oct-2008
NLCD 2008	26-Oct-2008
NLCD 2006	18-Oct-2005
BICM 2005	17-Nov-2005
NLCD 2004	15-Oct-2004
BICM 2004	20-Jan-2004
NLCD 2001	17-Jun-2001; 15-Oct-2001
BICM 1998	24-Jan-1998

Table S4. Confusion matrices showing results of accuracy assessment comparing the water, bare earth (sand), and vegetated classes from land-cover datasets generated in this study with temporally consistent NLCD and BICM datasets at the northern Chandeleur Islands. [Abbreviations: User_A, user's accuracy; Producer_A, producer's accuracy]

	Reference Dataset: BICM 2016					
Classed Data: 17-Nov-2016	Class	Water	Bare Earth	Vegetated	Total	User_A
	Water	100	0	0	100	100.0%
	Bare Earth	36	57	7	100	57.0%
	Vegetated	32	3	65	100	65.0%
	Total	168	60	72	300	
	Producer_A	59.5%	95.0%	90.3%		74.0%

	Reference Dataset: NLCD 2016					
Classed Data: 17-Nov-2016	Class	Water	Bare Earth	Vegetated	Total	User_A
	Water	98	1	1	100	98.0%
	Bare Earth	12	69	19	100	69.0%
	Vegetated	48	11	41	100	41.0%
	Total	158	81	61	300	
	Producer_A	62.0%	85.2%	67.2%		69.3%

	Reference Dataset: BICM 2016					
Classed Data: 18-Jan-2016	Class	Water	Bare Earth	Vegetated	Total	User_A
	Water	97	0	1	100	97.0%
	Bare Earth	28	43	5	100	43.0%
	Vegetated	23	4	71	100	71.0%
	Total	176	47	77	300	
	Producer_A	56.3%	91.5%	92.2%		71.0%

	Reference Dataset: NLCD 2016					
Classed Data: 18-Jan-2016	Class	Water	Bare Earth	Vegetated	Total	User_A
	Water	98	0	2	100	98.0%
	Bare Earth	12	72	16	100	72.0%
	Vegetated	22	7	71	100	71.0%
	Total	132	79	89	300	
	Producer_A	74.2%	91.1%	79.8%		80.3%

	Reference Dataset: NLCD 2013					
Classed Data: 24-Oct-2013	Class	Water	Bare Earth	Vegetated	Total	User_A
	Water	97	3	0	100	97.0%
	Bare Earth	30	42	28	100	42.0%
	Vegetated	21	3	76	100	76.0%
	Total	148	48	104	300	
	Producer_A	65.5%	87.5%	73.1%		71.7%

Table S4. Confusion matrices showing results of accuracy assessment—continued.

Classed Data: 03-Oct-2011

Reference Dataset: NLCD 2011

Class	Water	Bare Earth	Vegetated	Total	User_A
Water	100	0	0	100	100.0%
Bare Earth	10	59	31	100	59.0%
Vegetated	22	2	76	100	76.0%
Total	132	61	107	300	
Producer_A	75.8%	96.7%	71.0%		78.3%

Classed Data: 30-Jan-2009

Reference Dataset: BICM 2008

Class	Water	Bare Earth	Vegetated	Total	User_A
Water	97	0	0	100	97.0%
Bare Earth	14	50	10	100	50.0%
Vegetated	26	2	61	100	61.0%
Total	177	52	71	300	
Producer_A	56.5%	96.2%	85.9%		70.3%

Classed Data: 30-Jan-2009

Reference Dataset: NLCD 2008

Class	Water	Bare Earth	Vegetated	Total	User_A
Water	97	2	1	100	97.0%
Bare Earth	82	7	11	100	7.0%
Vegetated	36	1	63	100	63.0%
Total	215	10	75	300	
Producer_A	45.1%	70.0%	84.0%		55.7%

Classed Data: 18-Oct-2005

Reference Dataset: NLCD 2006

Class	Water	Bare Earth	Vegetated	Total	User_A
Water	95	1	4	100	95.0%
Bare Earth	49	6	45	100	6.0%
Vegetated	44	4	52	100	52.0%
Total	188	11	101	300	
Producer_A	50.5%	54.5%	51.5%		51.0%

Classed Data: 18-Oct-2005

Reference Dataset: BICM 2005

Class	Water	Bare Earth	Vegetated	Total	User_A
Water	98	0	2	100	98.0%
Bare Earth	46	0	47	100	0.0%
Vegetated	46	0	52	100	52.0%
Total	199	0	101	300	
Producer_A	49.2%	0.0%	51.5%		50.0%

Table S4. Confusion matrices showing results of accuracy assessment—continued.

Classed Data: 15-Oct-2004

Reference Dataset: NLCD 2004

Class	Water	Bare Earth	Vegetated	Total	User_A
Water	97	2	1	100	97.0%
Bare Earth	48	34	18	100	34.0%
Vegetated	53	6	41	100	41.0%
Total	198	42	60	300	
Producer_A	49.0%	81.0%	68.3%		57.3%

Classed Data: 31-Mar-2004

Reference Dataset: BICM 2004

Class	Water	Bare Earth	Vegetated	Total	User_A
Water	94	0	4	100	94.0%
Bare Earth	24	64	3	100	64.0%
Vegetated	29	4	66	100	66.0%
Total	159	68	73	300	
Producer_A	60.4%	94.1%	90.4%		75.3%

Classed Data: 21-Sep-2001

Reference Dataset: NLCD 2001

Class	Water	Bare Earth	Vegetated	Total	User_A
Water	100	0	0	100	100.0%
Bare Earth	20	75	5	100	75.0%
Vegetated	54	8	38	100	38.0%
Total	174	83	43	300	
Producer_A	57.5%	90.4%	88.4%		71.0%

Classed Data: 17-Feb-1998

Reference Dataset: BICM 1998

Class	Water	Bare Earth	Vegetated	Total	User_A
Water	93	0	4	100	93.0%
Bare Earth	24	61	5	100	61.0%
Vegetated	19	12	66	100	66.0%
Total	152	73	75	300	
Producer_A	63.2%	83.6%	88.0%		74.3%

Table S5. Confusion matrices showing results of accuracy assessment comparing the water, bare earth (sand), vegetated, and intertidal classes from land-cover datasets generated in this study with temporally consistent BICM datasets at the northern Chandeleur Islands. [Abbreviations: User_A, user's accuracy; Producer_A, producer's accuracy]

	Reference Dataset: BICM 2016					
Classed Data: 17-Nov-2016	Class	Water	Bare Earth	Vegetated	Intertidal	Total	User_A
	Water	100	0	0	0	100	100.0%
	Bare Earth	23	57	7	13	100	57.0%
	Vegetated	20	3	65	12	100	65.0%
	Intertidal	63	5	7	25	100	25.0%
	Total	206	65	79	50	400	
	Producer_A	48.5%	87.7%	82.3%	50.0%		61.8%[1]

	Reference Dataset: BICM 2016					
Classed Data: 18-Jan-2016	Class	Water	Bare Earth	Vegetated	Intertidal	Total	User_A
	Water	97	0	1	2	100	97.0%
	Bare Earth	28	43	5	24	100	43.0%
	Vegetated	23	4	71	2	100	71.0%
	Intertidal	32	10	25	33	100	33.0%
	Total	180	57	102	61	400	
	Producer_A	53.9%	75.4%	69.6%	54.1%		61.0%[1]

	Reference Dataset: BICM 2008					
Classed Data: 30-Jan-2009	Class	Water	Bare Earth	Vegetated	Intertidal	Total	User_A
	Water	97	0	0	3	100	97.0%
	Bare Earth	14	50	10	26	100	50.0%
	Vegetated	26	2	61	11	100	61.0%
	Intertidal	35	4	3	58	100	58.0%
	Total	172	56	74	98	400	
	Producer_A	56.4%	89.3%	82.4%	59.2%		66.5%

	Reference Dataset: BICM 2005					
Classed Data: 18-Oct-2005	Class	Water	Bare Earth	Vegetated	Intertidal	Total	User_A
	Water	98	0	2	0	100	98.0%
	Bare Earth	46	0	47	7	100	0.0%
	Vegetated	46	0	52	2	100	52.0%
	Intertidal	69	0	18	13	100	13.0%
	Total	259	0	119	22	400	
	Producer_A	37.8%	0.0%	43.7%	59.1%		40.8%

	Reference Dataset: BICM 2004					
Classed Data: 31-Mar-2004	Class	Water	Bare Earth	Vegetated	Intertidal	Total	User_A
	Water	94	0	4	2	100	94.0%
	Bare Earth	24	64	3	9	100	64.0%
	Vegetated	29	4	66	1	100	66.0%
	Intertidal	48	11	11	30	100	30.0%
	Total	195	79	84	42	400	
	Producer_A	48.2%	81.0%	78.6%	71.4%		63.5%

Table S5. Confusion matrices showing results of accuracy assessment—continued.

	Reference Dataset: BICM 1998					
Classed Data: 17-Feb-1998	Class	Water	Bare Earth	Vegetated	Intertidal	Total	User_A
	Water	93	0	4	3	100	93.0%
	Bare Earth	24	61	5	10	100	61.0%
	Vegetated	19	12	66	3	100	66.0%
	Intertidal	24	35	35	6	100	6.0%
	Total	160	108	110	22	400	
	Producer_A	58.1%	56.5%	60.0%	27.3%		56.5%

Table S6. Land-cover areas ($m^2 \times 10^3$) for the entire northern Chandeleur Islands study area averaged for time periods corresponding to natural (storm) and anthropogenic (berm construction) events that affected historical land-cover changes (Figure 2). Single-factor Analysis of Variance (ANOVA) comparing land-cover extents for successive analysis periods were significant ($p < 0.01$) for all comparisons except for comparison of intertidal extents for 1984-1998 compared with 1999-2005 ($p = 0.74$) and comparison of vegetated extents for 2005-2010 compared with 2010-2019 ($p = 0.09$).

Time Period	Bare Earth (Sand)	Vegetated	Total Island[1]	Intertidal	Barrier Platform[2]
1984-1998 (pre-Georges)	4561.4 ± 896.3	10636 ± 1455.3	15197.4 ± 1582.8	8470.7 ± 2842.4	23668.2 ± 3186
1999-2005 (pre-Katrina)	3274 ± 665.7	7208.9 ± 975.8	10482.8 ± 1275.7	8177.9 ± 3389.9	18660.7 ± 4182.6
2005-2010 (post-Katrina)	1279.9 ± 426.1	2265.3 ± 580.3	3545.2 ± 530.6	4084.8 ± 1679.5	7630 ± 1827.2
2010-2019 (post-berm)	3249.6 ± 730.4	2925.8 ± 964.9	6175.5 ± 1269.3	9772.3 ± 1942.6	15947.8 ± 2289.7

[1]Sand plus vegetated extents
[2]Sand plus vegetated plus intertidal extents

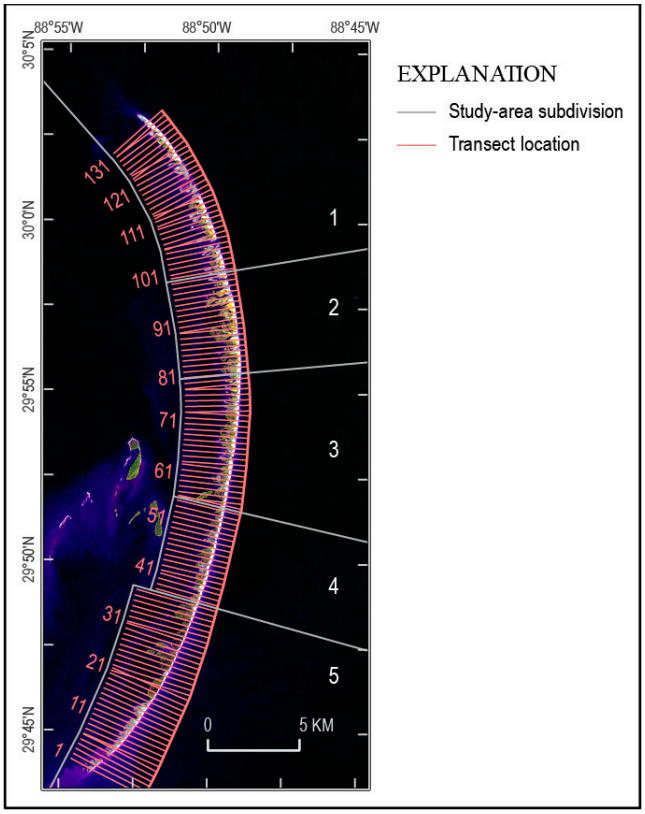

Figure S1. Study-area map showing cross-shore transects used to calculate barrier metrics and shoreline-change rates along the northern Chandeleur Islands. False-color Landsat 5 satellite image acquired 25-Mar-1984 is overlaid with study-area subdivisions; display uses bands 4,5,3.

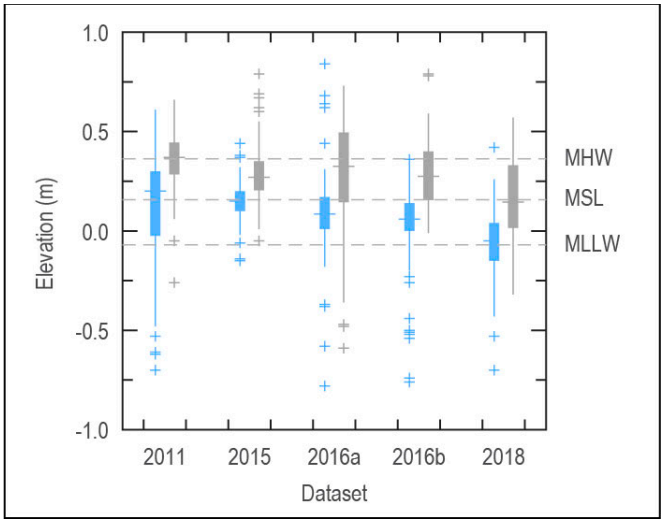

Figure S2. Boxplot showing distribution of elevations extracted from temporally consistent lidar datasets for intertidal "submerged" (blue boxes) and intertidal "emergent" (gray boxes) subclasses at the northern Chandeleur Islands. Dataset comparisons are 2011: 21-Feb-2011 Landsat 5 classed image with Feb-2011 lidar; 2015: 20-Mar-2015 Landsat 8 classed image with Feb-2015 lidar; 2016a: 6-Mar-2016 Landsat 8 source image with Jun-2016 lidar; 2016b: 22-Mar-2016 Landsat 8 classed image with Jun-2016 lidar; 2018: 10-Jan-2019 Landsat 8 classed image with Oct-2018 lidar. [Abbreviations: MLLW, mean lower low water; MSL, mean sea level; MHW, mean high water]

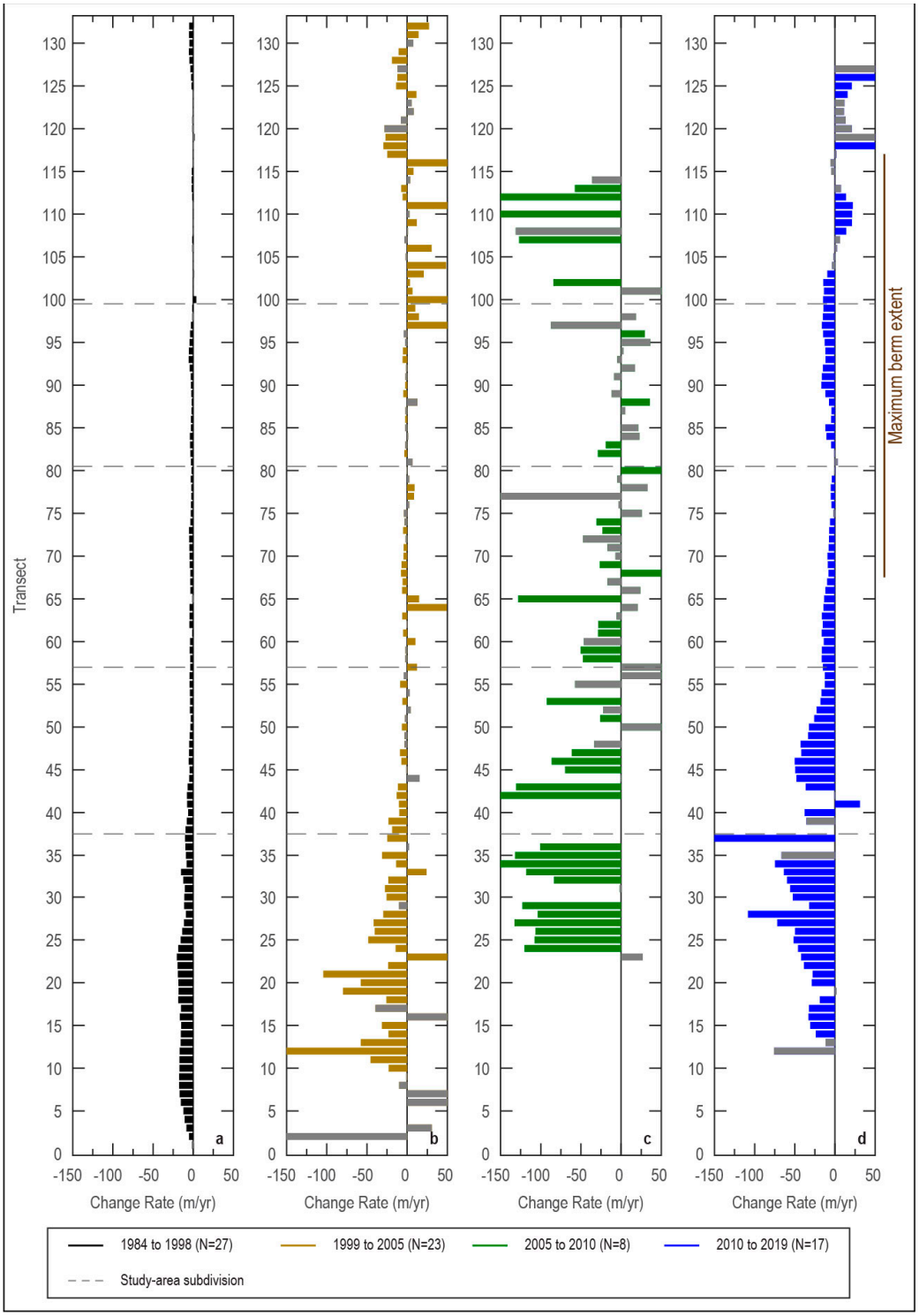

Figure S3. Linear-regression shoreline-change rates along cross-shore transects spaced 300 m alongshore at the northern Chandeleur Islands for (a) 25-Mar-1984 to 22-Apr-1998 (pre-Hurricane Georges), (b) 10-Jan-1999 to 24-Mar-2005 (pre-Hurricane Katrina), (c) 18-Oct-2005 to 18-Feb-2010 (post Hurricane Katrina), and (d) 3-Dec-2010 to 19-Jan-2019 (post-berm construction). Gray bars indicate rates for which $p > 0.05$. Dashed horizontal lines indicate study area subdivision boundaries. Rates for bars that extend beyond axis limits are labeled.

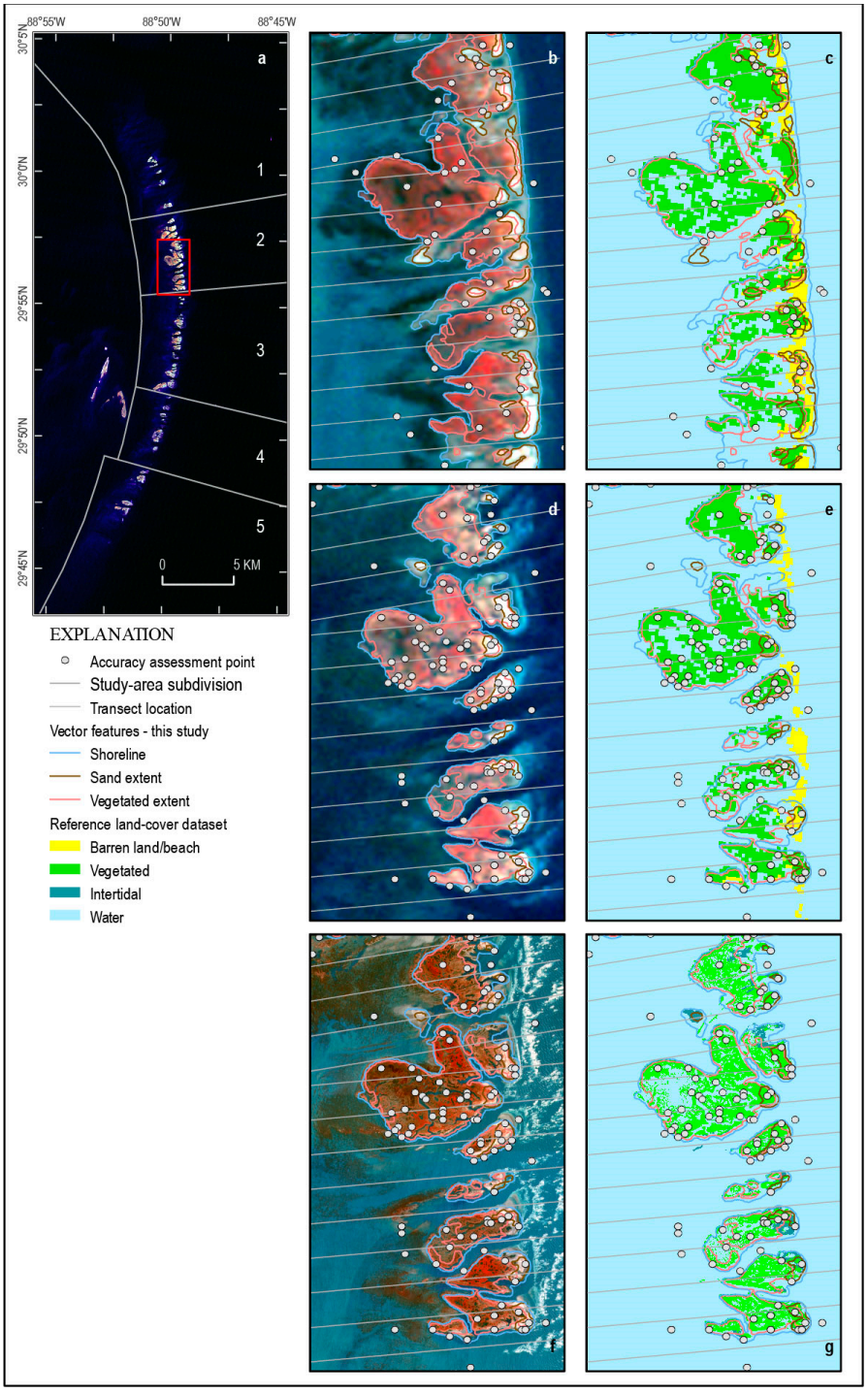

Figure S4. (a) Map of the northern Chandeleur Islands study area; inset boxes show location of panels b-e. False-color Landsat 5 satellite image acquired 18-Oct-2005 is overlaid with study-area subdivisions. (b-e) Vector feature extents show location of mapped barrier-platform and sand extents from Landsat 5 image acquired 18-Oct-2005 and randomly generated accuracy-assessment points compared to (b) Landsat 5 satellite image acquired 15-Oct-2004, (c) NLCD 2004 reference dataset, (d) Landsat 5 satellite image acquired 18-Oct-2005, (e) NLCD 2006 reference dataset, (f) BICM 2005 source color-infrared aerial imagery acquired 17-Nov-2005, and (g) BICM 2005 reference dataset. False-color images use bands 4,3,2 (Landsat) or 4,1,2 (aerial imagery).

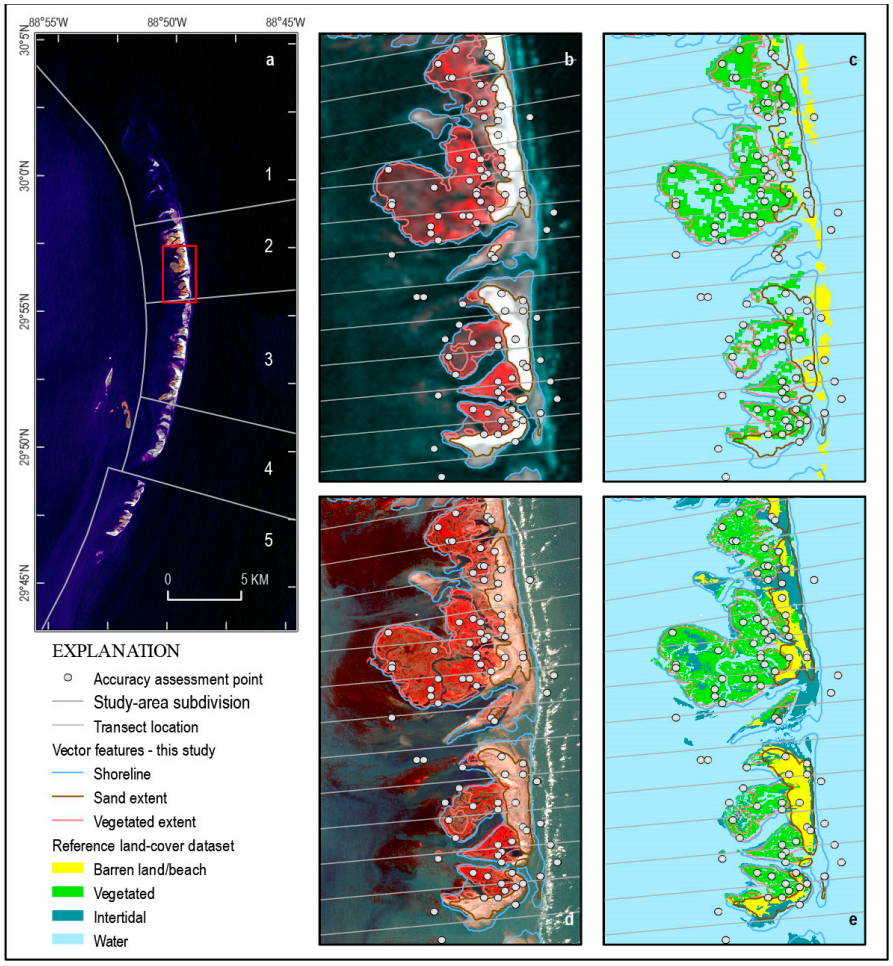

Figure S5. (a) Map of the northern Chandeleur Islands study area; inset boxes show location of panels b-e. False-color Landsat 5 satellite image acquired 30-Jan-2009 is overlaid with study-area subdivisions. (b-e) Vector feature extents show location of mapped barrier-platform and sand extents from Landsat 5 image acquired 30-Jan-2009 and randomly generated accuracy-assessment points (compared to (b) Landsat 5 satellite image acquired 30-Jan-2009, (c) NLCD 2008 reference dataset, (d) BICM 2008 source color-infrared aerial imagery acquired 28- and 29-Oct-2008, and (e) BICM 2008 reference dataset. False-color images use bands 4,3,2 (Landsat) or 4,1,2 (aerial imagery).

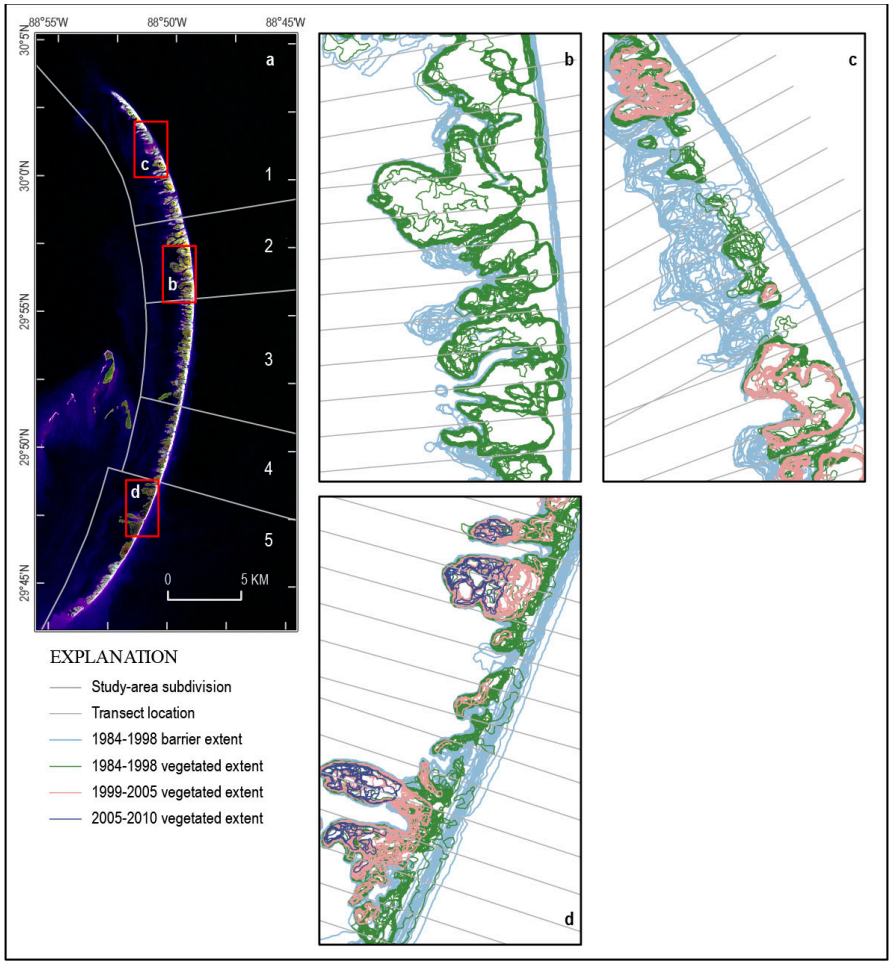

Figure S6. (a) Map of the northern Chandeleur Islands study area; inset boxes show location of panels b-d. False-color Landsat 5 satellite image acquired 25-Mar-1984 is overlaid with study-area subdivisions; display uses bands 4,5,3. Vector feature extents demonstrate (b) relative stability of the mapped back-barrier platform behind the stable marsh platform in subarea 2; (c) vegetation loss along a narrow, low persistence vegetated flat following Hurricane Georges; and (d) erosion and narrowing of the vegetated platform through landward erosion of the seaward edge.

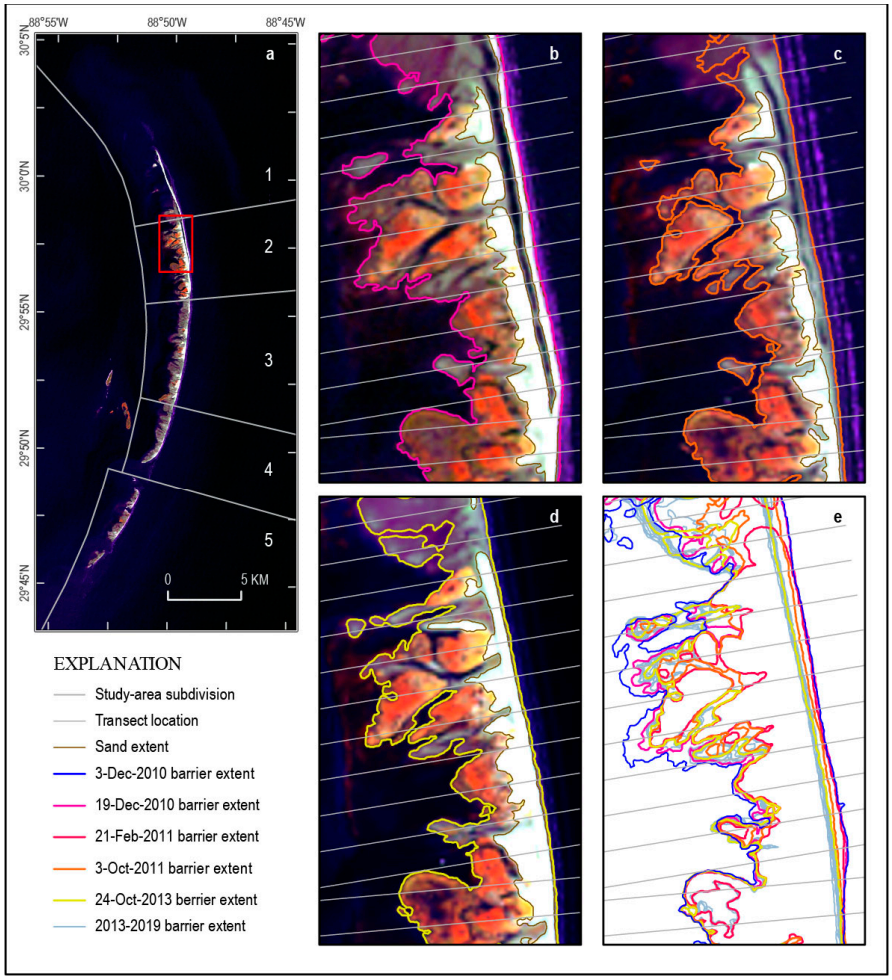

Figure S7. (a) Map of the northern Chandeleur Islands study area; inset box shows location of panels b-e. Landsat 5 satellite image acquired 19-Dec-2010 is overlaid with study-area subdivisions. (b-d) Vector feature extents show location of mapped barrier-platform and sand extents from Landsat 5 images acquired (b) 19-Dec-2010, (c) 3-Oct-2011 and (d) Landsat 8 image acquired 24-Oct-2013. (e) Vector barrier-platform extents demonstrate rapid landward translation of emplaced berm sediment between Dec-2010 and Oct-2011 and comparatively stable sea shoreline position since 2013. False-color images use bands 4,5,3 (Landsat 5) or 5,6,3 (Landsat 8).

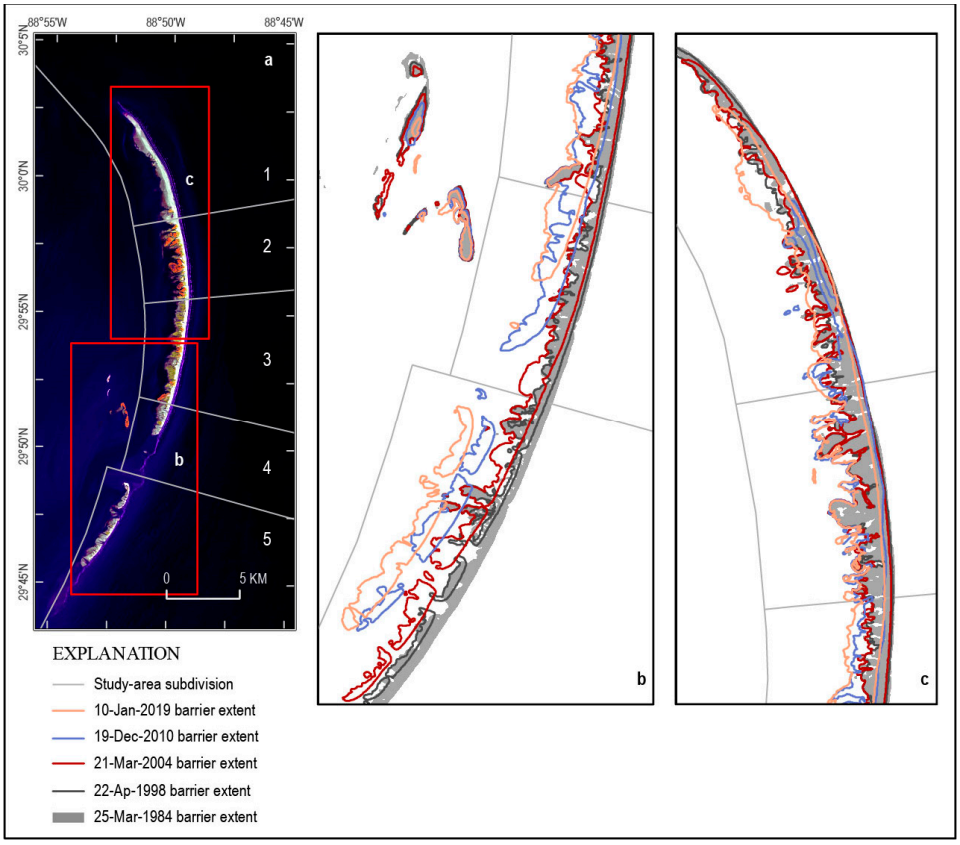

Figure S8. (a) Map of the northern Chandeleur Islands study area; inset box shows location of panels b-c. Landsat 5 satellite image acquired 19-Dec-2010 is overlaid with study-area subdivisions. Vector barrier-platform extents demonstrate (b) landward translation of the post-1984 barrier platform relative to the historical (1984) barrier footprint in the southern part of the study area and (c) relative stability of the barrier platform location in the central study area where backed by a persistent vegetated platform. In the northern study area (c), the barrier platform remerged after 2010, but mostly within the historical barrier footprint.